

Adaptive Continuously Variable Compression Braking Control for Heavy-Duty Vehicles

Maria Druzhinina
Anna Stefanopoulou

Mechanical Engineering Department,
University of Michigan,
Ann Arbor, MI 48197

Lasse Moklegaard
Mechanical and Environmental
Engineering Department,
University of California,
Santa Barbara, CA 93106

Modern heavy-duty vehicles are equipped with compression braking mechanisms that augment their braking capability and reduce wear of the conventional friction brakes. In this paper we consider a heavy-duty vehicle equipped with a continuously variable compression braking mechanism. The variability of the compression braking torque is achieved through controlling a secondary opening of the exhaust valve of the vehicle's turbocharged diesel engine using a variable valve timing actuator. A model reference adaptive controller is designed to ensure good vehicle speed tracking performance in brake-by-wire driving scenarios in presence of large payload and road grade variations. The adaptive controller is integrated with backstepping procedure to account for compression braking actuator dynamics, with observers for various unmeasured quantities and with compensation schemes for actuator saturation. In addition to speed tracking, the vehicle mass and road grade are simultaneously estimated if persistence of excitation-type conditions hold. The final version of the controller is successfully evaluated on a high order crank angle model of a vehicle with a six-cylinder engine.

[DOI: 10.1115/1.1486010]

1 Introduction

Increased highway capacity and enhanced driving safety (which are the major goals for Automated Highway Systems [1–3]) impose fundamental requirements on retarding power and braking control of modern Heavy Duty Vehicles (HDVs). Although, conventional service brakes (friction pads on the wheels) can theoretically provide a retarding power ten times higher than the accelerating power of the vehicle, they cannot be used continuously because of the generated heat that may cause “brake fading” and excessive wear of the friction contacts [4]. The presence of delays associated with the pneumatic or the hydraulic actuation subsystem impose additional constraints on the longitudinal control of HDVs [5]. To maintain operational speeds comparable to passenger vehicles, without compromising safe braking performance, high retarding power with consistent magnitude and unlimited duration is required. Faced with these difficulties, fleet and engine manufacturers are introducing additional retarding mechanisms with low weight and maintenance requirement so they do not offset the recent improvements in powertrain efficiency.

A promising retarding mechanism that satisfies the above low maintenance and weight-to-power ratio requirements is the engine compression brake that relies on converting the turbocharged diesel engine, that powers HDVs, into a compressor that absorbs kinetic energy from the crankshaft [6,7]. It is based on inhibiting fuel injection and altering the conventional gas exchange process in the cylinders of the engine through a secondary opening of the exhaust valve at the end of the compression stroke. We call the secondary opening of the exhaust valve when the air is released into the exhaust as Brake Valve Opening (BVO) (or braking event) and we refer to the corresponding timing of the exhaust valve opening as Brake Valve Timing (BVT). Specifically, we define BVT as the number of crank angle degrees from the top-dead-center at the beginning of the power stroke to the opening of the brake valve, as shown in Fig. 1.

Variability of the compression braking torque can be achieved by (a) varying the brake valve timing using a variable exhaust

camshaft phasing actuator, (b) varying the number of cylinders that are operating under compression mode. With the latter version of the compression braking mechanism only a finite number of possible braking torque values can be achieved for a given engine speed. The number of possible discrete torque values depends on the number of cylinders activated in compression mode. The finest quantization of engine braking torque that can be achieved with this approach is defined by the number of cylinders of the engine. A further quantization of the braking torque delivered to the wheels can be achieved through the gear selection in the driveline. Thus, the request of negative torque can be approximately matched by combining a certain number of “braking” cylinders and a certain choice of gear ratio. This capability is utilized in the Eaton-Vorad collision-warning system EVT-300 with SmartCruise that activates compression braking automatically when a collision is imminent. It is not clear, however, that a vehicle following can be realized, unless the service brakes that are normally controlled by the driver can smoothly compensate for the compression braking torque deficit at a given speed. The stringent requirements of HDV following scenarios and other applications in Intelligent Transportation necessitate continuous variation in the compression braking torque. Thus, continuously variable compression braking achieved through a continuous variation in brake valve timing (option (a)) is currently under active investigation [8]. This is the type of actuator that we focus on in our paper.

To study the effects of the continuously varying brake valve timing we developed a detailed crank angle based model appropriate for longitudinal control of a typical Class 8 highway truck equipped with compression brake. The model accurately represents the transient and nonlinear behavior of the engine and the vehicle during combustion and braking modes, and during the transition between those modes [9]. Applying numerical model order reduction techniques to this model we have developed a set of low order models that can be used for control analysis and design [10].

In this paper, we concentrate on the longitudinal speed control problem using only variable compression braking in an effort to increase HDV retarding capability, accommodate higher operating speeds and minimize the use of the conventional friction brake and, hence, the friction brake wear. To ensure good and consistent

Contributed by the Dynamic Systems and Control Division for publication in the JOURNAL OF DYNAMIC SYSTEMS, MEASUREMENT, AND CONTROL. Manuscript received by the Dynamic Systems and Control Division March 1, 2000. Associate Editor: S. Sivashankar.

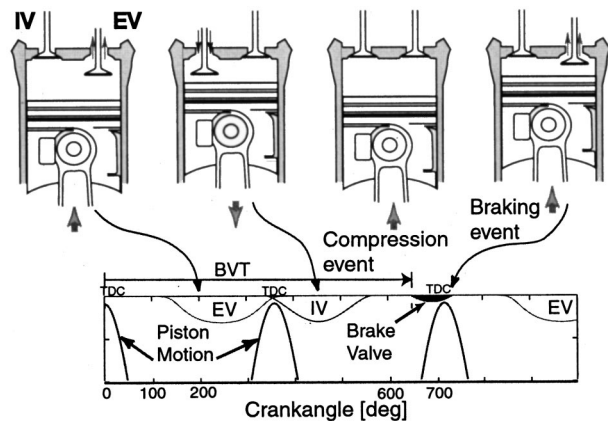


Fig. 1 Lift profiles for exhaust, intake and brake events

speed tracking performance despite large variations in the vehicle mass and road grade, we pursue an adaptive control approach. We first consider the model without compression brake actuator dynamics and derive a Model Reference Adaptive Controller in terms of system parameter estimates [11]. The update laws for the parameter estimates are generated using the Speed-Gradient technique [12]. Then the actuator dynamics are accounted for in the controller design through the use of a backstepping procedure. The backstepping controller is implemented using observers for various unmeasured variables and the stability of the scheme is rigorously analyzed. We, furthermore, outline several ways to deal with actuator saturation. Finally, the scheme developed on a simplified model is successfully applied to a high order crankangle based model of a diesel engine equipped with a compression braking actuator [13]. In order to compensate for undesirable effects of the high order model such as cylinder-to-cylinder interactions, we employ additional measures to enhance our scheme robustness. Specifically, the dead-zone and adaptation disabling in fast transients are introduced to deal with unmodeled dynamics. Their effect is to stop adaptation when the unmodeled dynamics are dominant. Good tracking performance and identifying properties of the final version of the controller for vehicle mass and road grade are demonstrated on crankangle based engine model simulation.

The paper is organized as follows. In the immediately following section we review the key issues and challenges of longitudinal control of HDVs and summarize the related literature and the contribution of our paper. In Section 3 we describe a model for longitudinal vehicle dynamics and compression braking actuator dynamics. In Section 4 we develop a Model Reference Adaptive Controller (MRAC) assuming, first, the instantaneous actuator response. We then extend the control design to the case with the actuator dynamics. In Section 5 we consider different approaches to deal with the actuator saturation. We then introduce modifications to enhance the control scheme robustness. With these modifications the controller is successfully applied to the full order model and the results are reported in Section 6. Concluding remarks follow in Section 7.

2 Challenges in Longitudinal Control and Parameter Estimation of HDVs

To guarantee safe and reliable operation of automated vehicles, modern speed control systems are designed to provide good speed tracking performance and robustness for a multitude of operating conditions such as vehicle mass, road grade, gear combinations, aerodynamic drag, etc. A sensitivity analysis of the HDV model variations (see [10,14]) clearly indicates that more sophisticated control schemes have to be introduced to meet the stringent performance requirements. The issue of vehicle load changes is of particular concern in HDV, since the HDV's mass can vary as

much as 400 percent (from a configuration of being just a tractor to having one or more trailers) resulting in drastically different closed loop performance. The experiments on an HDV [15] indicate that the conventional controllers, such as a fixed gain PID, have limited capability to handle the large parameter variations of HDV. Road grade changes are the second most important issue that present strong challenges, especially combined with uncertainties in the vehicle mass.

A very promising approach to enhance the conventional control algorithms is that of on-line parameter estimation and controller adaptation. Several adaptive algorithms related to automotive speed control applications have been introduced in prior literature (see, e.g., [16–21]). In particular, in [16] the authors develop an optimization-type direct adaptation algorithm that adjusts the gains of a PI controller to minimize a cost functional that reflects vehicle performance objectives over varying road conditions. The authors of [17] use an indirect adaptive scheme with the recursive least-squares method to identify parameters in a linearized vehicle model. A least-square estimator that provides vehicle mass, aerodynamic drag and rolling resistance estimates is described in [18]. It can be used to implement algorithms for indirect adaptive control. Adaptive algorithms have been developed in [19] to address unpredictable changes in parameters of conventional service brakes. Recent work [20] shows that nonsmooth estimation and adaptation techniques can be used to achieve a reasonable control over braking force of conventional service brakes.

The first results on adaptive longitudinal control design for HDV are presented in [5,21]. There the authors develop an adaptive controller for an HDV with conventional friction brakes using the direct adaptation of PIQ controller gains. The novelty of our work is in using an indirect adaptive control method applied directly to nonlinear longitudinal vehicle dynamics model and compression braking actuation mechanism. In particular, a Model Reference Adaptive Controller is derived in terms of two system parameter estimates, namely vehicle mass and road grade [11]. Both of these parameters are found to be critical in longitudinal control since they have the most impact on the longitudinal performance [14].

In addition to speed tracking we are also able, under persistence of excitation type conditions, to estimate *simultaneously* vehicle mass and road grade. We show that the convergence of these two estimates is assured when the desired speed value changes in a step-wise or other periodic fashion (that is typically guaranteed in urban driving cycles).

Reliable on-line HDV parameter estimation has a large impact for reducing emissions, increasing fuel efficiency and enhancing safety of automated vehicles. In light of HDV automation an accurate payload mass estimation is critical for implementing a control scheme proposed in [14], where reference commands to individual trucks are adjusted so that all trucks in a platoon can follow the reference command from the leading truck without saturating their actuators. Moreover, estimation of payload mass in HDVs is very important and it is used nowadays by fueling algorithms to reduce smoke and by the transmission shift strategy to eliminate “gear hunting.” An electronically controlled HDV powertrain can accomplish online mass parameter estimation using two primary methods: (a) acceleration data during a step change in fueling rate, (b) acceleration or deceleration data during a gear shift. In all of these methods, changes in road grade confuse the mass estimation algorithms by biasing the driveline torque that is available for acceleration or deceleration. Method (b) is more accurate because it does not depend on a feedforward steady-state combustion torque estimator that is prone to errors due to engine aging. However, it is expected that shift duration will be shortened in the future to reduce speed loss and consequently smoke emission generation during gear shifts, and, thus, method (b) will be increasingly difficult to apply for parameter estimation. Grade information can be potentially obtained using road map information and satellite communication. In [14] a two-antenna GPS system is

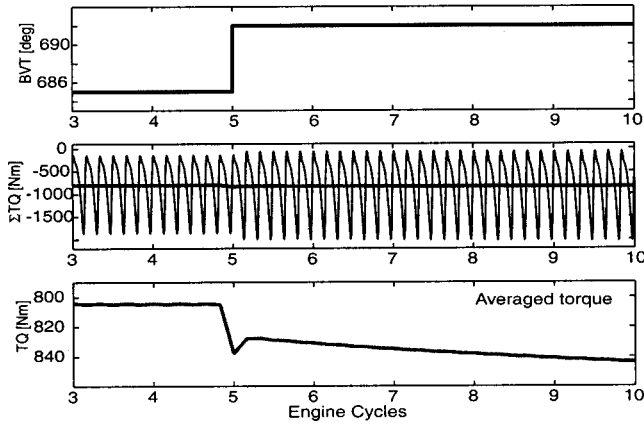


Fig. 2 The instantaneous shaft torque response to a step change in BVT from 685 deg to 692 deg. The third plot shows the event-averaged torque response. Source: [10].

used for road grade measurements within a least-square based estimation scheme. The adaptive scheme proposed in this paper provides mass and road grade estimation without any additional sensors or measurements, but it is limited by the fact that the estimation happens only during compression braking periods.

3 Longitudinal Vehicle Model

Consider the vehicle operation during a driving maneuver on a descending grade with β degrees inclination ($\beta=0$ corresponds to no inclination, $\beta<0$ corresponds to a descending grade). It is assumed that during the descent, the engine is not fueled and is operated in the compression braking mode. A lumped parameter model approximation is used to describe the vehicle longitudinal dynamics during compression braking. For fixed gear operation the engine crankshaft rotational speed, ω , is expressed by:

$$J_t \dot{\omega} = T_{cb} + r_g (F_\beta - F_{qdr}), \quad (1)$$

where T_{cb} is the engine torque applied to the crankshaft (negative during compression braking), $J_t = Mr_g^2 + J_e$ is the total vehicle inertia reflected to the engine shaft, J_e is the engine crankshaft inertia, M is the mass of the vehicle (depends on the mass of payload). The total gear ratio, r_g , is given by $r_g = r_\omega / g_t g_{fd}$, where r_ω is the wheel diameter, g_t is the transmission gear ratio, g_{fd} is the final drive gear ratio. F_{qdr} is the quadratic resistive force (primarily, force due to aerodynamic resistance, but we also include friction resistive terms):

$$F_{qdr} = C_q r_g^2 \omega^2,$$

where $C_q = C_d A \rho / 2 + C_f$ is the quadratic resistive coefficient, C_d is the aerodynamic drag coefficient, ρ is ambient air-density, A is the frontal area of the vehicle and C_f is the friction coefficient. F_β is the force due to road grade (β) and the rolling resistance of the road (f_r):

$$F_\beta = -f_r g M \cos \beta - M g \sin \beta,$$

where g is the acceleration due to gravity. The engine speed ω is proportional to the vehicle speed v , i.e., $v = \omega r_g$, as long as the gear ratio remains constant.

In [9] we have developed a detailed crank angle based model for the compression braking torque. This high-order dynamic model is based on energy conservation principles in addition to static engine maps provided by the manufacturers, and it is capable of describing the intrinsic interactions between individual cylinder intake and exhaust processes, and turbocharger dynamics during combustion and braking modes and during the transition between the modes (see the crank angle based model simulation for a step change in BVT from 685 deg to 692 deg in Fig. 2).

Based on averaging and identification of the instantaneous torque response for changes in brake valve timing and engine speed, a low order control oriented engine model has been derived in [10]. The lower plot in Fig. 2 shows the cycle-averaged torque response obtained by processing the summation of individual cylinder torque in the crank angle domain (middle plots) with a third order Butterworth filter. The cutoff frequency corresponds to one engine cycle.

The reduced model is essentially represented as follows. The compression braking torque on the crankshaft, T_{cb} , is calculated using the following first order differential equation with the time constant $1/\lambda_{cb}$:

$$\dot{T}_{cb} = -\lambda_{cb}(T_{cb} - T_{st}), \quad (2)$$

where the steady-state braking torque, T_{st} , is calculated as a nonlinear function of the engine speed ω and the brake valve timing u_{cb} :

$$T_{st}(\omega, u_{cb}) = \alpha_0 + \alpha_1 \omega + \alpha_2 u_{cb} + \alpha_3 u_{cb} \omega. \quad (3)$$

The regression (3) has been obtained in [10] by fitting the simulation results from the full order model. The brake valve timing limits impose limits on the braking torque $T_{st, \min}(\omega) = T_{st}(u_{cb, \max}, \omega)$, $T_{st, \max}(\omega) = T_{st}(u_{cb, \min}, \omega)$.

Recent developments in the area of high pressure valve actuation hydraulics (see e.g., [8]) allow us to assume that the actuator opening the brake valve is considerably faster than the engine manifold filling and turbocharger dynamics. Thus, the brake valve timing u_{cb} can be treated as a control input. The controller in this paper is designed directly in terms of torque T_{st} from (2) through backstepping, while the corresponding value of the brake valve timing, u_{cb} , is obtained by inverting the static torque regression (3).

The speed control problem is to ensure that the engine rotational speed ω tracks the desired reference speed $\omega_d(t)$ as the vehicle proceeds the descending grade: $\omega \rightarrow \omega_d(t)$. This ensures that $v \rightarrow v_d(t)$ as long as the gear ratio remains constant. We assume that the desired speed $\omega_d(t)$ is derived from the driver's brake pedal position through a calibration map. These calibration maps are typically developed by skilled drivers and can be used in a brake-by-wire mode. In Automated Highway Systems (AHS) the value of $\omega_d(t)$ may be generated from a lead vehicle.

4 Model Reference Adaptive Controller

The sensitivity analysis and, in particular, significant variations in the vehicle response characteristics to an application of compression brake clearly indicate the need for nonlinear and adaptive control design to ensure good and consistent HDV speed tracking performance for a multitude of vehicle mass, road grade and gear combinations [10]. The design of such nonlinear adaptive controller is the topic of this section. Specifically, we develop a Model Reference Adaptive Controller that is derived in terms of two system parameter estimates, namely vehicle mass and road grade. Both of these parameters are found to be critical in longitudinal control since they have the most impact on longitudinal performance [14].

The design of the controller algorithm is first done for the system without the actuator dynamics. The actuator dynamics need to be taken into account if higher levels of performance (e.g., faster response, disturbance rejection) are desired from the closed loop system. In Subsection 4.3 we extend the controller algorithm to account for the actuator dynamics. The simulation results on the reduced order model in Subsection 4.4 provide the benchmark performance for comparison controller performance on the full order model in the following sections.

4.1 Controller Design Without the Actuator Dynamics.

We assume that the mass m of the vehicle (which depends on the mass of payload) and the road grade β are unknown constants. This implies that the total vehicle inertia $J_t(m)$ and the force

$F_\beta(m, \beta)$ due to road grade (β) and the rolling resistance of the road (f_r) are unknown constants as well. Then the vehicle model in the parametric form is

$$\dot{\omega} = \frac{1}{\theta_1} (u - r_g^3 C_q \omega^2 + \theta_2), \quad (4)$$

where u is the shaft torque T_{cb} , and θ_1, θ_2 are unknown parameters, $\theta_1 = J_t > 0$, $\theta_2 = r_g F_\beta$. Note that θ_1 , which is the total vehicle inertia, is always positive. This property is critical to being able to develop a MRAC design.

To design MRAC we introduce a reference model that captures the desired closed-loop behavior. Specifically, the reference model trajectory ω_m is given by

$$\dot{\omega}_m = -\lambda \omega_m + \lambda \omega_d, \quad (5)$$

where $\omega_d(t)$ is the desired vehicle speed and $\lambda > 0$ controls the speed of response, whereby larger values of λ correspond to faster responses. The speed reference model approach is particularly suitable for operating trucks in a vehicle following scheme within an AHS environment because heavy vehicle response should not vary too much when operating conditions change to avoid adverse effect on traffic flow.

Denoting the tracking error by $e = \omega - \omega_m$, we obtain:

$$\dot{e} = \frac{1}{\theta_1} (u - r_g^3 C_q \omega^2 + \theta_2) + \lambda \omega_m - \lambda \omega_d. \quad (6)$$

Using the certainty equivalence principle, we define the feedback law as follows:

$$u = r_g^3 C_q \omega^2 - \theta_2 - \theta_1 \lambda (\omega - \omega_d). \quad (7)$$

If θ_1, θ_2 were known, this controller would guarantee that $e(t) \rightarrow 0$. Since the parameters are unknown, we replace them by their estimates, $\hat{\theta}_1, \hat{\theta}_2$, in the control law (7):

$$u = r_g^3 C_q \omega^2 - \hat{\theta}_2 - \hat{\theta}_1 \lambda (\omega - \omega_d). \quad (8)$$

The parameters $\hat{\theta}_1, \hat{\theta}_2$ will be adjusted by the adaptation law. The error model is given by:

$$\dot{e} = -\lambda e + \theta_1^{-1} \lambda (\omega - \omega_d) (\theta_1 - \hat{\theta}_1) + \theta_1^{-1} (\theta_2 - \hat{\theta}_2). \quad (9)$$

The parameter update laws are derived using the Speed Gradient methodology [12]. This is a general technique for controlling nonlinear systems through an appropriate selection and minimization of a goal function. The controller is designed to provide a decrease in the goal function along the trajectories of the system. The goal function Q is selected to reflect the speed tracking objective, specifically: $Q(e) = \theta_1 e^2 / 2 \geq 0$. Note that $Q(e) > 0$ if $e \neq 0$ because $\theta_1 > 0$. Then,

$$\dot{Q} = -\lambda \theta_1 e^2 + e \lambda (\omega - \omega_d) (\theta_1 - \hat{\theta}_1) + e (\theta_2 - \hat{\theta}_2),$$

and in accordance with the SG approach, we calculate the derivative of \dot{Q} with respect to $\hat{\theta}_1$ and $\hat{\theta}_2$ (the gradient of the "speed") and define the following adaptation laws:

$$\dot{\hat{\theta}}_1 = -\gamma_1 \nabla_{\hat{\theta}_1} \dot{Q} = \gamma_1 e \lambda (\omega - \omega_d), \quad \gamma_1 > 0, \quad (10)$$

$$\dot{\hat{\theta}}_2 = -\gamma_2 \nabla_{\hat{\theta}_2} \dot{Q} = \gamma_2 e, \quad \gamma_2 > 0, \quad (11)$$

where $\gamma_1, \gamma_2 > 0$ are positive adaptation gains. The convergence $e(t) \rightarrow 0$ can be proved using the following Lyapunov function:

$$V(e, \tilde{\theta}) = Q(e) + \frac{1}{2\gamma_1} \tilde{\theta}_1^2 + \frac{1}{2\gamma_2} \tilde{\theta}_2^2 \geq 0, \quad (12)$$

where $\tilde{\theta} = [\tilde{\theta}_1 \tilde{\theta}_2]^T$, and $\tilde{\theta}_i = \theta_i - \hat{\theta}_i$, $i = 1, 2$. Calculating the time derivative of V , using the adaptation laws (10)–(11), we obtain

$$\dot{V} = -\lambda \theta_1 e^2 \leq 0.$$

Thus $V(e(t), \tilde{\theta}(t))$ is a non-increasing function of time and $V(e(t), \tilde{\theta}(t)), Q(e(t))$ are bounded. Then, $e(t), \tilde{\theta}(t)$ are also bounded. From (9), assuming that $\omega_d(t), t \geq 0$, is bounded, $\dot{e}(t), t \geq 0$, is bounded as well. The Barbalat's lemma can now be applied to show that $e(t) \rightarrow 0$, i.e., $\omega(t) \rightarrow \omega_m(t)$, as $t \rightarrow \infty$. Note that if $\omega_d(t) \equiv \omega_d = \text{const}$ for $t \geq t'$, $\omega(t) \rightarrow \omega_d$.

To ensure that the parameter estimates are bounded within a realistic feasible range and to improve the parameter estimate transient behavior we can augment a projection algorithm to (10)–(11). Suppose $\theta_{1,\min} \leq \theta_1 \leq \theta_{1,\max}, \theta_{2,\min} \leq \theta_2 \leq \theta_{2,\max}$. The parameter updates are stopped if $\hat{\theta}_1, \hat{\theta}_2$ attempt to leave their respective feasible intervals:

$$\dot{\hat{\theta}}_1 = Proj_1[\gamma_1 e \lambda (\omega - \omega_d), \hat{\theta}_1], \quad (13)$$

$$\dot{\hat{\theta}}_2 = Proj_2[\gamma_2 e, \hat{\theta}_2], \quad (14)$$

where for $i = 1, 2$,

$$Proj_i[x, y] = \begin{cases} 0, & \text{if } x \geq 0, y \geq \theta_{i,\max} \\ 0, & \text{if } x \leq 0, y \leq \theta_{i,\min} \\ x, & \text{otherwise} \end{cases}$$

When the projection is employed, the time-derivative of V has the form:

$$\dot{V} = -\lambda \theta_1 e^2 + \Phi, \quad (15)$$

where

$$\Phi \triangleq \tilde{\theta}_1 (e \lambda (\omega - \omega_d) - Proj_1[e \lambda (\omega - \omega_d), \hat{\theta}_1]) + \tilde{\theta}_2 (e - Proj_2[e, \hat{\theta}_2]). \quad (16)$$

From $\theta_{i,\min} \leq \theta_i \leq \theta_{i,\max}$, and definition of $Proj_i$ it is straightforward to verify that $\Phi \leq 0$, and hence, $e(t), \tilde{\theta}(t)$ remain bounded. Assuming that $\omega_d(t), t \geq 0$, is bounded, the uniform continuity of $e^2(t), t \geq 0$, follows from boundedness of $\dot{e}(t)$ in (9). Hence, the convergence $e(t) \rightarrow 0$ as $t \rightarrow \infty$ follows from the Barbalat's lemma.

4.2 On-line Parameter Estimation. We next study the identifying properties of our algorithm and demonstrate that our control scheme will provide mass and road grade estimation under additional persistence of excitation type conditions. Specifically, if parameter convergence $\hat{\theta}_1(t) \rightarrow \theta_1, \hat{\theta}_2(t) \rightarrow \theta_2$ as $t \rightarrow \infty$ takes place then accurate estimates of the mass m and of the road grade β can be backtracked from $\hat{\theta}_1$ and $\hat{\theta}_2$. The error model (9) can be rewritten in the form:

$$\theta_1 \dot{e} = -\lambda \theta_1 e + R^T \tilde{\theta}, \quad (17)$$

where $R = [\lambda (\omega - \omega_d) \ 1]^T$ is the regressor function, $\tilde{\theta} = [\tilde{\theta}_1 \ \tilde{\theta}_2]^T$. From $e(t) \rightarrow 0$, (13), (14) it follows that $\tilde{\theta}(t) \rightarrow 0$ as $t \rightarrow \infty$. Using the Barbalat's lemma we can show that $\dot{e}(t) \rightarrow 0$ as well. From (17) this implies that $R(t)^T \tilde{\theta}(t) \rightarrow 0$ as $t \rightarrow \infty$. Suppose $\omega_d(t) \equiv \text{const}$ for $t \geq t'$. Then, $\omega(t) - \omega_d(t) \rightarrow 0$ as $t \rightarrow \infty$ and $\tilde{\theta}_2(t) \rightarrow 0$ as $t \rightarrow \infty$. Unfortunately, the convergence of $\hat{\theta}_2$ does not allow us to simultaneously identify both the road grade and the vehicle mass. To obtain both the convergence $\tilde{\theta}_2(t) \rightarrow 0$ and $\tilde{\theta}_1(t) \rightarrow 0$ as $t \rightarrow \infty$, $\omega_d(t)$ should not be constant, and additional conditions on $R(t)$ are needed. Specifically, the matrix $R(t)$ must be persistently exciting [22]. In practice, this persistent excitation condition can be enforced if ω_d is not a constant and provides a sufficiently rich excitation to the system, e.g., changes in a stepwise or other periodic fashion. This is typically guaranteed in urban driving cycles.

4.3 Including Compression Braking Dynamics. We further extend the design to include the brake actuator dynamics (2). The system with the actuator dynamics is given by:

$$J_t \dot{\omega} = T_{cb} + r_g (-C_q r_g^2 \omega^2 + F_\beta) \quad (18)$$

$$\dot{T}_{cb} = -\lambda_{cb}(T_{cb} - T_{st}), \quad (19)$$

where T_{st} is now considered as a control input. The higher order controller that takes the actuator dynamics in (2) into account is designed using a backstepping approach [23]. In accordance with this iterative design procedure we have to treat T_{cb} as a virtual input to the first-order system (18) and, as a first step, design a stabilizing control law $\alpha(e, \hat{\theta}_1, \hat{\theta}_2)$ for (18) and the update laws for $\hat{\theta}_1, \hat{\theta}_2$. This, in fact, has already been done in the previous section and

$$\alpha(e, \hat{\theta}_1, \hat{\theta}_2) = r_g^3 C_q \omega^2 - \hat{\theta}_2 - \hat{\theta}_1 \lambda (\omega - \omega_d). \quad (20)$$

The error between T_{cb} and α is denoted by $z = T_{cb} - \alpha(e, \hat{\theta}_1, \hat{\theta}_2)$. To account for this error, we augment the Lyapunov function (12) with the term $1/2z^2$:

$$V_{a1}(e, z, \tilde{\theta}_1, \tilde{\theta}_2) = V(e, \tilde{\theta}_1, \tilde{\theta}_2) + \frac{1}{2}z^2. \quad (21)$$

The time-derivative of V_{a1} along the trajectories of the closed-loop system (18), (19), (20), (13), (14) is given by

$$\begin{aligned} \dot{V}_a &= \theta_1 e \dot{e} - \gamma_1^{-1} \tilde{\theta}_1 \dot{\theta}_1 - \gamma_2^{-1} \tilde{\theta}_2 \dot{\theta}_2 + z(\dot{T}_{cb} - \dot{\alpha}) \\ &= -\theta_1 \lambda e^2 + \Phi + z(e - \lambda_{cb}(T_{cb} - T_{st}) - \dot{\alpha}). \end{aligned} \quad (22)$$

Therefore, to guarantee negative definiteness of \dot{V}_{a1} we need to choose T_{st} to make the last term of (22) equal to $-kz$, where $k > 0$ is a controller gain. This is achieved with the following control law:

$$T_{st} = T_{cb} + \lambda_{cb}^{-1}(-kz - e + \dot{\alpha}), \quad (23)$$

where

$$\dot{\alpha} = (2C_q r_g^3 \omega - \hat{\theta}_1 \lambda) \dot{\omega} - \lambda(\omega - \omega_d) \dot{\theta}_1 - \dot{\theta}_2 + \hat{\theta}_1 \lambda \dot{\omega}_d. \quad (24)$$

Since $z = T_{cb} - \alpha$,

$$T_{st} = (1 - k\lambda_{cb}^{-1})T_{cb} - \lambda_{cb}^{-1}(e - k\alpha - \dot{\alpha}). \quad (25)$$

Note that (23) (or (25)) depend on several quantities that we do not measure directly. In particular, the control law (25) depends on the time derivative of ω which is not measured (unless there is an accelerometer on-board). Therefore, to make the above controller implementable, we have to introduce an approximation of the derivative operator (so called "dirty derivative" [5], which is given by a transfer function $s/(s/\tau + 1)$, $\tau > 0$) for $\dot{\omega}$. Then the control law (25) is modified as follows:

$$\begin{aligned} T_{st} &= (1 - k\lambda_{cb}^{-1})T_{cb} - \lambda_{cb}^{-1}(e - k\alpha - \hat{\alpha}) \\ \alpha &= r_g^3 C_q \omega^2 - \hat{\theta}_2 - \hat{\theta}_1 \lambda (\omega - \omega_d), \\ \hat{\alpha} &= (2C_q r_g^3 \omega - \hat{\theta}_1 \lambda) \dot{\omega}_f - \lambda(\omega - \omega_d) \hat{\theta}_1 - \hat{\theta}_2 + \hat{\theta}_1 \lambda \dot{\omega}_d \\ \dot{\omega}_f &= \tau(\omega - \omega_f), \\ \hat{\theta}_1 &= Proj_1[\gamma_1 e \lambda (\omega - \omega_d), \hat{\theta}_1], \\ \hat{\theta}_2 &= Proj_2[\gamma_2 e, \hat{\theta}_2]. \end{aligned} \quad (26)$$

The analysis of this controller algorithm with the dirty derivative approximation is presented in the Appendix. The properties of the original algorithm are essentially recovered if $\gamma_1, \gamma_2, k, \tau$ are sufficiently large. The backstepping procedures that rely on the dirty derivative approximation are analyzed in [24] for the non-adaptive case. From these non-adaptive results, we would expect that k and τ need to be sufficiently large. As is shown in the Appendix, in the adaptive case, the adaptation gains need also be sufficiently high.

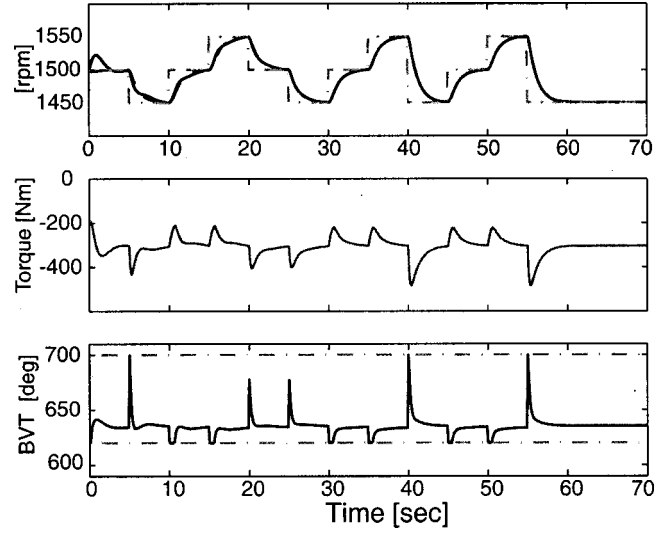


Fig. 3 Upper plot: engine speed ω (solid) in response to desired speed ω_d (dash-dot) and reference model trajectory ω_m (dash). Lower plots: the trajectories of torque T_{cb} and brake valve timing u_{cb} (solid). $u_{cb,max}$, $u_{cb,min}$ are indicated by dash-dotted lines.

We also do not measure the shaft torque T_{cb} . To estimate T_{cb} , we may use an open-loop observer,

$$\hat{T}_{cb} = -\lambda_{cb}(\hat{T}_{cb} - T_{st}).$$

The estimate \hat{T}_{cb} replaces T_{cb} in the control law (25). Because the solution of $\dot{e}_{cb} = -\lambda_{cb}e_{cb}$, where $e_{cb} = \hat{T}_{cb} - T_{cb}$ exponentially converges to zero, it can be verified that the algorithm properties are preserved with this observer. Note that the effectiveness of the open-loop observer depends on knowing accurately the value of λ_{cb} . The use of this open-loop observer can be avoided altogether in vehicles equipped with a torque sensor, where T_{cb} would be directly measured. There may also be alternative procedures for estimating T_{cb} from the driveline/transmission side that also avoid using the open-loop observer. In our case the actual braking torque, that exhibits higher frequency content, was neglected by the open loop observer model. Despite the unmodeled high order dynamics we confirm in Section 6 that the speed tracking performance and parameter error reduction are maintained even during simulation with the full order model.

4.4 Simulation Results on Reduced Order Model. To illustrate the operation of our adaptive controller given by (27) and (3), we consider a response to a desired vehicle speed profile ω_d , given by a step-wise periodic function that slightly exaggerates an urban driving scenario. The vehicle operates in fifth gear. The initial parameter estimates are 60 percent off the true values of the mass and grade, thus resulting in poor tracking performance (see Fig. 3). The tracking improves as the adaptation proceeds. During this particular periodic excitation in ω_d the vehicle mass and road grade estimates tend to their true values in 35 s as shown in Fig. 4. The variations in the engine speed in Fig. 6 correspond to variations in the desired vehicle speed between 18.3 km/h and 19.6 km/h. This is a very small variation in the vehicle speed that would be hardly noticeable to the driver. In fact, this excitation may be imposed artificially by the control system on top of the nominal desired vehicle speed set by the driver.

These results are obtained under the assumption that the regression (3) is accurate. Simulations using a perturbed model of steady-state torque \hat{T}_{st} demonstrates a reasonable sensitivity to the regression errors. For example, a 10 percent persistent mismatch caused by multiplicative uncertainty between the modeled and

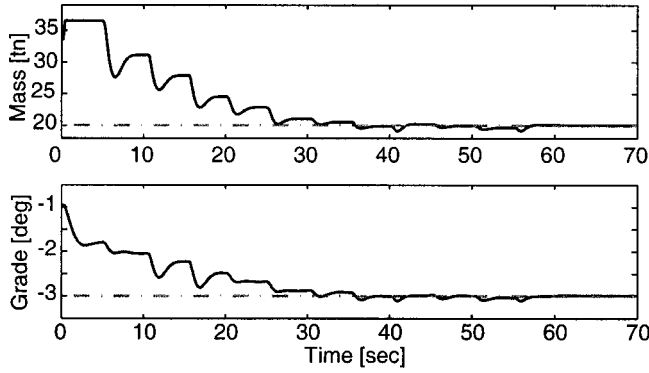


Fig. 4 Convergence of vehicle mass and road grade parameter estimates. The true values are given by the dash-dotted lines, the estimates by the solid lines.

actual torque ($\hat{T}_{st} = 1.1T_{st}$) results in 10 percent steady-state error in the estimate of the vehicle mass and 1 percent error in the estimate of the road grade. Note that the speed tracking performance does not deteriorate even in the presence of this modeling error.

5 Saturation Compensation Schemes

Since the range of brake valve opening timing is limited, actuator saturation may occur. From Fig. 3 we note that u_{cb} saturates during transients (the saturation limits are indicated by dash-dotted lines). The closed loop controller responses may diverge if the saturation is not properly handled. The actuator saturation can be handled within the control design in two different ways described below.

5.1 Reference Modification. To provide compensation for actuator saturation we use the approach of [25]. The idea is to preserve the time-rate of decay of the Lyapunov function even if saturation is encountered by properly modifying the reference command. Unlike in [25], here we apply the scheme to an adaptive system.

The reference model (5), that captures the desired closed loop behavior, is modified as follows:

$$\dot{\omega}_m = \lambda(\omega_m - \omega_{d,f}). \quad (27)$$

The signal $\omega_{d,f}$ is calculated as an output of the following filter with a time constant τ_d :

$$\dot{\omega}_{d,f} = \tau_d(\omega_d - \omega_{d,f}) + r, \quad (28)$$

where $r(t)$ is a reference signal modification that is chosen to provide the same \dot{V}_a in saturation as when there is no saturation. Taking into account the new reference model (27)–(28), we obtain the following adaptation laws:

$$\hat{\theta}_1 = \gamma_1 Proj_1[e\lambda(\omega - \omega_{d,f}), \hat{\theta}_1], \quad \gamma_1 > 0. \quad (29)$$

$$\hat{\theta}_2 = \gamma_2 Proj_2[e, \hat{\theta}_2], \quad \gamma_2 > 0. \quad (30)$$

The above approach for saturation compensation is tested through simulation (see Fig. 5) during a driving maneuver in the gear number seven. Note that although saturation occurs in Fig. 3, the duration is not sufficiently long to test the modification (28). In the seventh gear, the reference modification scheme is active during the last downward step in ω_d from 1550 rpm to 1350 rpm (that corresponds to 32.5 km/h and 28.5 km/h, respectively). One can observe that the virtual reference $\omega_{d,f}$ is slowed down substantially as compared to ω_d to allow the system to catch up with the command. The controller scheme including the reference modification performed well for all the driving scenarios we tested through simulations. The theoretical analysis of the closed-

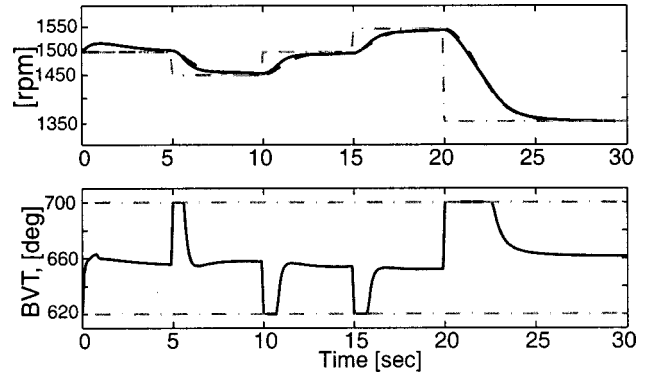


Fig. 5 Upper plot: engine speed ω (solid) in response to desired speed $\omega_{d,f}$ (dash-dot) and reference model trajectory ω_m (dash). Lower plot: the trajectories of brake valve timing u_{cb} (solid). $u_{cb,max}$, $u_{cb,min}$ are indicated by dash-dotted lines.

loop properties for this more complex scheme with saturation compensation will be reported in the future work.

5.2 Coordination With Gear. In order to avoid actuator saturation, an alternative approach can be used. Specifically, if the limits of the compression braking torque are frequently reached, a different transmission gear ratio can be selected. With an appropriate gear ratio selection one can effectively “size” the power due to gravity that is reflected on the engine shaft, see (1). The selection of the transmission gear ratio, g_t , would typically be done by a higher level supervisory controller if a frequent saturation of brake valve timing is detected. The control algorithm we have developed in the previous sections can be extended to include gear ratio optimization and selection. A similar gear selection scheme has been developed in [26].

6 Adaptive Controller Implementation on Full Order Model

In this section we test our adaptive controller on the high order crank-angle based engine model (with 24 dynamic states) for a six cylinder, 350 Hp diesel engine equipped with a compression brake. The high order engine model was developed in [9]. The crank angle representation allows us to capture the cylinder-to-cylinder interactions and individual cylinder variables such as pressure, temperature and torque in crank angle resolution during the transition from combustion to braking. The high frequency content of the quasi-periodic crank angle resolved cylinder operation may affect the controller operation and lead to closed-loop performance deterioration (e.g., see the oscillations in the braking torque produced by the cyclic operation of engine cylinders shown in Fig. 2). In order to compensate for undesirable effects of the high order model that we expect to be present in the real world system, we develop the following controller modifications that guarantee robust controller performance and improved parameter convergence.

In order to improve robustness of the adaptation and estimation algorithms, various modifications have been reported in the literature (see [27, 22] for a survey). For our application we already employed the feasible range projection algorithm wherein the parameter updates are stopped if the parameter estimates attempt to leave the region where the parameters are known to physically lie in (see Section 4.1). This approach is suitable for our application since the physically reasonable parameter range is typically known a priori.

Additional steps for improved parameter convergence consist of keeping the adaptation on only when the tracking error $\omega - \omega_m$ is expected to be due to parameter mismatch and not due to unmodeled dynamics effects or measurement noise. Thus the adaptation is turned off during fast transients, when the engine speed is

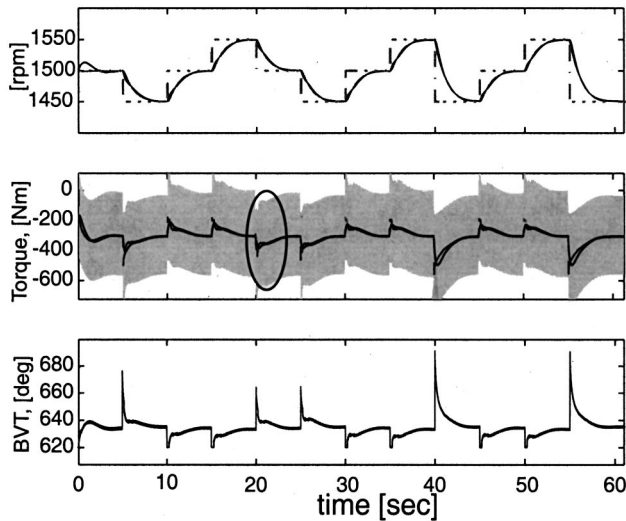


Fig. 6 Upper plot: engine speed ω (solid) in response to desired speed ω_d (dash-dot) and reference model trajectory ω_m (dash). Second plot: the trajectories of instantaneous, averaged and estimated shaft torque T_{cb} . Lower plot: brake valve timing trajectory.

changing fast, and modeling errors between the actual averaged torque and the estimated one are expected. The conditions for disabling adaptation in transients were formulated based on the difference between ω_d and ω_m . Namely, when this difference was smaller than a threshold in absolute value we enabled the adaptation. The threshold was tuned in simulations. A more systematic approach would involve defining disable conditions based on a difference between ω and a moving average of ω . We also turn the adaptation off when the tracking error $\omega - \omega_m$ is smaller than the measurement error or the quasi-steady periodic error in the torque caused by cylinder-to-cylinder operation (see Fig. 2). An upper bound on the uncertainty (that determines the size of the dead zone) can be derived from the crank angle engine dynamics model analysis.

To illustrate the operation of the adaptive controller, we consider the response to a desired vehicle speed profile ω_d given by the same step-wise periodic function used in Subsection 4.4. The large parameter errors (in particular, the initial parameter error of 60 percent) result in initially poor tracking performance (see Fig. 6). The tracking rapidly improves as the adaptation proceeds. During this particular periodic excitation in ω_d the errors in vehicle mass and road grade estimates reduce by more than a half in 35 sec as shown in Fig. 7. Because of the unmodeled dynamics

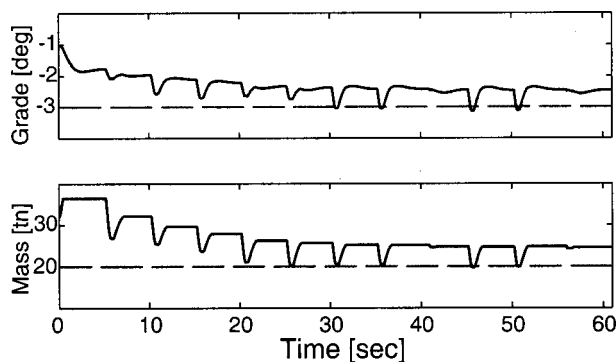


Fig. 7 The convergence of vehicle mass and road grade parameter estimates. The true values are given by the dashed lines, the estimates by the solid lines.

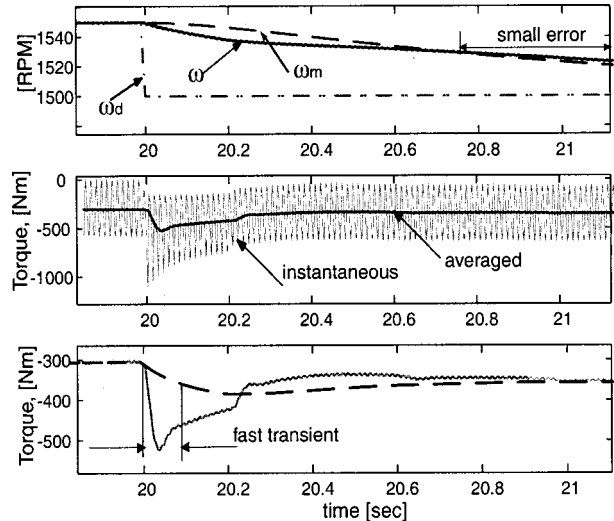


Fig. 8 Upper plot: engine speed ω in response to desired speed ω_d and reference model trajectory ω_m . Second plot: the trajectories of instantaneous and averaged shaft torque T_{cb} . Lower plot: averaged torque (solid) and estimated torque T_{cb} (dash).

present in the full order model, the parameter estimation error is not reduced to zero unlike in simulations on the reduced order model. Despite the unmodeled dynamics, the reduction in the parameter error is quite significant and our prime objective, which is good and consistent speed tracking performance, is achieved. The two regions where the adaptation is disabled (i.e., in fast transients and dead zone) are clearly visible in Fig. 8, which magnifies the signals during the step change at $t=20$ s indicated by a circle in Fig. 6.

7 Conclusion

In this paper we developed longitudinal speed control algorithms using variable compression braking in an effort to increase HDV retarding capability, accommodate higher operating speeds and lower maintenance cost due to reduced use of service brakes. To ensure good and consistent speed tracking performance despite large variations in the vehicle mass and road grade, the controller was integrated with on-line adaptation. A Model Reference Adaptive Control design approach combined with backstepping to include the compression braking actuator dynamics was followed. Observers for the unmeasured quantities have been designed and integrated with the baseline adaptive controller. The stability and response properties of the overall scheme have been rigorously analyzed. Several modifications for robust performance were considered. The final version of the controller was evaluated on the highly complex crank angle based model. Good tracking performance and parametric error reduction for vehicle mass and road grade estimation have been confirmed.

We focused on speed tracking under large uncertainties in vehicle mass and road grade. There is an additional, but smaller, uncertainty in the compression braking torque regression. In fact, compression braking torque can be predicted more accurately than combustion torque [9] and this is in part why we are proposing to estimate vehicle mass and road grade during the time when the compression brake is active. Thus our approach is to deal with the largest uncertainty sources first and handle smaller uncertainty sources through robustification mechanisms such as a dead zone and transient disable. Our work can be also extended to consider fast varying road grade as in [28].

Acknowledgments

This research is supported in part by the California Department of Transportation through the California PATH Program under MOU 372 and MOU 393; matching funds are provided by Mack Trucks, Inc.

Appendix

We now analyze the properties of the adaptive control algorithm (27) in more detail. In particular, we show that the introduction of the dirty derivative approximation for the time derivative of ω does not destroy the desirable properties of the adaptive control scheme.

The expression for $\dot{\alpha}$ (24) can be written in the form

$$\dot{\alpha} = \sigma \dot{\omega} + \rho,$$

where

$$\sigma(\omega, \hat{\theta}_1) = (2C_d r_g^3 \omega - \hat{\theta}_1 \lambda),$$

$$\rho(\omega, \omega_d, \dot{\omega}_d, e, \hat{\theta}_1, \hat{\theta}_2) = -\lambda(\omega - \omega_d) \dot{\theta}_1 - \dot{\theta}_2 + \hat{\theta}_1 \lambda \dot{\omega}_d.$$

We have,

$$\hat{\alpha} = \sigma \dot{\omega}_f + \rho.$$

The control law

$$T_{st} = T_{cb} + \frac{1}{\lambda_{cb}} (-e + \hat{\alpha} - kz),$$

can be rewritten in the form

$$T_{st} = T_{cb} + \frac{1}{\lambda_{cb}} (-e + \dot{\alpha} - kz) - \frac{1}{\lambda_{cb}} \sigma(\dot{\omega} - \dot{\omega}_f).$$

Let

$$V_{a2} = V_{a1} + \frac{1}{2} (\omega - \omega_f)^2$$

$$= \frac{\theta_1}{2} e^2 + \frac{1}{2\gamma_1} \tilde{\theta}_1^2 + \frac{1}{2\gamma_2} \tilde{\theta}_2^2 + \frac{1}{2} z^2 + \frac{1}{2} (\omega - \omega_f)^2.$$

The time rate of change of V_{a2} along the trajectories of the closed-loop system is given by the following expression

$$\dot{V}_{a2} = -\theta_1 \lambda e^2 + \Phi - kz^2 - \tau(\omega - \omega_f)^2 + z\sigma(\tau(\omega - \omega_f) - \dot{\omega}).$$

In the closed-loop system the acceleration $\dot{\omega}$ is a function of the states, parameters and parameter estimates:

$$\dot{\omega} = \eta(z, \omega, \hat{\theta}_1, \hat{\theta}_2, \omega_d, \theta_1),$$

where

$$\eta(\dots) = \frac{1}{\theta_1} (z - \hat{\theta}_2 - \hat{\theta}_1 \lambda (\omega - \omega_d) + \theta_2).$$

Another way of representing V_{a2} is as a sum

$$V_{a2} = V_s + V_\theta,$$

where

$$V_s = \frac{\theta_1}{2} e^2 + \frac{z^2}{2} + \frac{(\omega - \omega_f)^2}{2}, \quad V_\theta = \frac{1}{2\gamma_1} \tilde{\theta}_1^2 + \frac{1}{2\gamma_2} \tilde{\theta}_2^2.$$

The function V_s can be viewed as the energy contained in the system state errors while V_θ can be viewed as the energy contained in the parameter errors.

Let

$$\epsilon(\gamma_1, \gamma_2) = \max_{\hat{\theta}, \theta \in [\theta_{1,\min}, \theta_{1,\max}] \times [\theta_{2,\min}, \theta_{2,\max}]} V_\theta.$$

Consider a sublevel set of V_s ,

$$\mathcal{C}_p = \{\phi: V_s(\phi) \leq p\}, \quad \text{where } \phi = (e, z, \omega - \omega_f).$$

Assume that the initial condition at time $t=0$ is $\phi(0) = (e(0), z(0), \omega(0) - \omega_f(0))$ such that $\phi(0) \in \mathcal{C}_p$, and, moreover,

$$|\omega_d(t)| + |\dot{\omega}_d(t)| \leq K_1, \quad t \geq 0,$$

where K_1 is known. In addition, we assume that $\omega_m(0) = \omega_d(0)$ and that from $|\omega_d(t)| + |\dot{\omega}_d(t)| \leq K_1$ it follows that $|\omega_m(t) - \omega_d(t)| \leq K_2$ for some $K_2 > 0$ and for all t . The existence of K_2 follows from the BIBO stability of the reference model.

The set defined by the inequalities

$$V_s(\phi) \leq p + \epsilon(\gamma_1, \gamma_2), \quad |\omega_m - \omega_d| \leq K_2, \quad |\omega_d| + |\dot{\omega}_d| \leq K_1$$

is compact and, hence, the continuous function $|\eta(z, \omega, \hat{\theta}_1, \hat{\theta}_2, \omega_d)|$ achieves a maximum on this set that we denote by η_1 . Similarly, the maximum of the function $|\sigma(\omega, \hat{\theta}_1) \eta(z, \omega, \hat{\theta}_1, \hat{\theta}_2, \omega_d)|$ over this set exists and is denoted by η_3 while that of $|\sigma(\omega, \hat{\theta}_1)|$ by η_2 . If $V_s(\phi) \leq p + \epsilon(\gamma_1, \gamma_2)$, we have

$$\dot{V}_{a2} \leq -\theta_1 \lambda e^2 + \Phi - kz^2 - \tau(\omega - \omega_f)^2 + |\omega - \omega_f| \eta_1 + \tau |z| |\omega - \omega_f| \eta_2 + |z| \eta_3.$$

Completing the squares, it can be verified that

$$\dot{V}_{a2} \leq -\theta_1 \lambda e^2 + \Phi - \frac{\tau}{2} (|\omega - \omega_f| - \eta_2 |z|)^2 + |z|^2 \left(\frac{\tau}{2} \eta_2^2 - \frac{k}{2} \right)$$

$$- \frac{\tau}{2} \left(|\omega - \omega_f| - \frac{\eta_1}{\tau} \right)^2 - \frac{k}{2} \left(|z| - \frac{\eta_3}{k} \right)^2 + \frac{\eta_1^2}{2\tau} + \frac{\eta_3^2}{2k}.$$

Denote

$$\beta(\phi) = -\frac{\tau}{2} \left(|\omega - \omega_f| - \frac{\eta_1}{\tau} \right)^2 - \frac{k}{2} \left(|z| - \frac{\eta_3}{k} \right)^2 + \frac{\eta_1^2}{2\tau} + \frac{\eta_3^2}{2k}$$

$$- \theta_1 \lambda e^2.$$

Then,

$$\dot{V}_{a2} \leq \beta(\phi).$$

Examining the expression for β , it is straightforward to verify that if k and τ are sufficiently large, $k > \eta_2^2 \tau$, then \dot{V}_{a2} is negative outside of a compact set $\mathcal{G}(\tau, k)$ in the interior of the set $\mathcal{C}_{p+\epsilon(\gamma_1, \gamma_2)}$. Specifically, we can select $\epsilon > 0$ sufficiently small and let $\mathcal{G}(\tau, k) = \mathcal{C}_{g(\tau, k)}$ where $\mathcal{C}_{g(\tau, k)-\epsilon}$ is the smallest sublevel set of V_s that contains all ϕ 's such that $\beta(\phi) > 0$ in its interior. Note that $\mathcal{G}(\tau, k)$ shrinks toward the origin as the gains k and τ are increased. In particular, we can assume that k and τ are sufficiently large so that $\mathcal{G}(\tau, k) \subset \mathcal{C}_{p+\epsilon(\gamma_1, \gamma_2)}$.

Applying the Barbalat's lemma it can be verified that the trajectory of $\phi(t)$ that starts with $\phi(0) \in \mathcal{C}_p$ must enter $\mathcal{G}(\tau, k)$ in a finite time. Unlike in the nonadaptive case once the trajectory enters $\mathcal{G}(\tau, k)$ it may not stay in it for all future time and, in fact, it may exit it at some later time. Specifically, when the trajectory is inside $\mathcal{G}(\tau, k)$, \dot{V}_{a2} may be positive. At the exit time instant, V_{a2} cannot exceed $g(\tau, k) + \epsilon(\gamma_1, \gamma_2)$. This implies, in turn, that after the first entry the trajectory of ϕ will always be confined to the sublevel set $\mathcal{C}_{g(\tau, k) + \epsilon(\gamma_1, \gamma_2)}$. It remains to point out that both $g(\tau, k)$ and $\epsilon(\gamma_1, \gamma_2)$ can be made arbitrary small by selecting τ , k , γ_1 and γ_2 sufficiently large and $k > \eta_2^2 \tau$.

To summarize, sufficiently large control gains combined with sufficiently fast adaptation rates can ultimately bound the tracking error e and approximation errors e_{cb} , z , $\omega - \omega_f$ within an arbitrary small compact set around the origin. The domain of attraction (i.e., the set of initial $\phi(0)$'s) for which this ultimate boundedness property holds can also be made arbitrary large by increasing the gains k and τ . Consequently, by utilizing large control gains and fast adaptation the desirable properties of our adaptive control

algorithm can be recovered despite the fact that a dirty derivative approximation for $\dot{\omega}$ are employed. The need to use fast adaptation is perhaps not surprising given the results on “bursting” prevention in adaptive control schemes in [29]. It can be also verified that if the persistence of excitation conditions hold and as long as ϕ is outside of $\mathcal{G}(\tau, k)$, the parameters converge exponentially to their true value.

References

- [1] Shladover, S. E., et al., 1991, “Automatic Vehicle Control Developments in the PATH Program,” *IEEE Trans. Veh. Technol.*, **40**(1), pp. 114–130.
- [2] Ioannou, P., and Chien, C. C., 1993, “Autonomous Intelligent Cruise Control,” *IEEE Trans. Veh. Technol.*, **42**, pp. 657–672.
- [3] Chen, C., and Tomizuka, M., 1995, “Steering and Independent Braking Control for Tractor-Semitrailer Vehicles in Automated Highway Systems,” *Proceedings of the 34th Conference on Decision and Control*, pp. 658–663.
- [4] Gerdes, J. C., Brown, A. S., and Hedrick, J. K., 1995, “Brake System Modeling for Vehicle Control,” *Advanced Automotive Technologies—ASME IMECE*, pp. 105–112.
- [5] Yanakiev, D., and Kanellakopoulos, I., 1997, “Longitudinal Control of Automated CHVs with Significant Actuator Delays,” *Proceedings of the 36th Conference on Decision and Control*, San Diego, pp. 4756–4763.
- [6] Cummins, D. D., 1966, “The Jacobs Engine Brake Application and Performance,” *SAE Paper No. 660740*.
- [7] Jacobs Vehicle System, 1999, “Intebrate Engine Braking System for Signature 600,” retrieved on <http://www.jakebrake.com/products/engine>.
- [8] Hu, H., Israel, M. A., and Vorih, J. M., 1997, “Variable Valve Actuation and Diesel Engine Retarding Performance,” *SAE Paper No. 970342*.
- [9] Moklegaard, L., Stefanopoulou, A., and Schmidt, J., 2000, “Transition from Combustion to Variable Compression Braking,” *SAE paper No. 2000-1-1228*.
- [10] Moklegaard, L., Stefanopoulou, A., and Druzhinina, M., 2000, “Brake Valve Timing and Fuel Injection: A Unified Engine Torque Actuator for Heavy-Duty Vehicles,” *Proc. of International Symposium on Advanced Vehicle Control*, Ann Arbor, Michigan.
- [11] Druzhinina, M., Moklegaard, L., and Stefanopoulou, A., 2000, “Compression Braking Control for Heavy-Duty Vehicles,” *Proceedings of American Control Conference*, Chicago, Illinois.
- [12] Fradkov, A. L., and Pogromsky, A. Yu., 1998, *Introduction to Control of Oscillations and Chaos*, World Scientific.
- [13] Druzhinina, M., Moklegaard, L., and Stefanopoulou, A., 2001, “Further Results on Adaptive Compression Braking Control for Heavy-Duty Vehicles,” *Advanced Automotive Technologies—ASME IMECE*, New York City.
- [14] Bae, H. S., and Gerdes, J. C., 2000, “Parameter Estimation and Command Modification for Longitudinal Control of Heavy Vehicles,” *Proc. of International Symposium on Advanced Vehicle Control*, Ann Arbor, MI.
- [15] Tan, Y., Robotis, A., and Kanellakopoulos, I., 1999, “Speed Control Experiments with an Automated Heavy Vehicle,” *Proceedings of the IEEE International Conference on Control Applications*, Hawaii, pp. 1353–1358.
- [16] Liubakka, M. K., Rhode, D. S., Winkelman, J. R., and Kokotovic, P. V., 1993, “Adaptive Automotive Speed Control,” *IEEE Trans. Autom. Control*, **38**(7), pp. 1011–1020.
- [17] Tsujii, M., Takeuchi, H., Oda, K., and Ohba, M., 1990, “Application of Self-Tuning to Automotive Cruise Control,” *Proceedings of the American Control Conference*, pp. 1843–1848.
- [18] Wuertemberger, M., Germann, S., and Isermann, R., 1992, “Modelling and Parameter Estimation of Nonlinear Vehicle Dynamics,” *ASME Dynamical Systems and Control Division*, Vol. DSC **44**, pp. 53–63.
- [19] Ioannou, P., and Xu, Z., 1994, “Throttle and Brake Control Systems for Automatic Vehicle Following,” *PATH Research Report UCB-ITS-PRR-94-10*.
- [20] Maciucu, D. B., and Hedrick, J. K., 1998, “Nonsmooth Estimation and Adaptive Control with Application to Automotive Brake Torque,” *Proceedings of American Control Conference*, pp. 2253–2257.
- [21] Yanakiev, D., and Kanellakopoulos, I., 1996, “Speed Tracking and Vehicle Follower Control Design for Heavy-Duty Vehicles,” *Veh. Syst. Dyn.*, **25**, pp. 251–276.
- [22] Ioannou, P., and Sun, J., 1996, *Robust Adaptive Control*, Prentice Hall, Englewood Cliffs, NJ.
- [23] Krstic, M., Kanellakopoulos, I., and Kokotovic, P. V., 1995, *Nonlinear and Adaptive Control Design*, Wiley, New York.
- [24] Swaroop, D., Gerdes, J. C., Yip, P. P., and Hedrick, J. K., 1997, “Dynamic Surface Control of Nonlinear Systems,” *Proceedings of the American Control Conference*, pp. 3028–3034.
- [25] Kang, J.-M., and Grizzle, J. W., 1999, “Nonlinear Control for Joint Air and Fuel Management in a SI Engine,” *Proceedings of the American Control Conference*.
- [26] Druzhinina, M., Moklegaard, L., and Stefanopoulou, A., 2000, “Speed Gradient Approach to Longitudinal Control of Heavy Duty Vehicles Equipped with Compression Brake,” *Proc. of International Symposium on Advanced Vehicle Control*, Ann Arbor, MI.
- [27] de Mathelin, M., and Lozano, R., 1999, “Robust Adaptive Identification of Slowly Time-Varying Parameters with Bounded Disturbances,” *Automatica*, **35**, pp. 1291–1305.
- [28] Druzhinina, M., Stefanopoulou, A., and Moklegaard, L., 2002, “Speed Gradient Approach to Longitudinal Control of Heavy-Duty Vehicles Equipped With Variable Compression Brake,” *IEEE Trans. on Control Systems Technology*, **10**(2), pp. 209–220.
- [29] Jankovic, M., 1996, “Adaptive Output Feedback Control of Non-linear Feedback Linearizable Systems,” *Int. Journal of Adaptive Control and Signal Processing*, **10**, pp. 1–18.